

Radiological impact of natural radioactivity and excessive lifetime cancer risk in Egyptian phosphate rocks along Red Sea, Egypt

E. S. AbdEl-Halim¹, AmanyTahaSroor^{1,*}, NadiaWalley El-Dine¹, Ibrahim E. El-Aassy², Enass M. El-Sheikh², NaimaM Al-kbashy³.

¹ Faculty of Women for Arts, Science and Education, Physics Department, Ain Shams University, Cairo, Egypt

² Nuclear Materials Authority, Cairo, Egypt

³ Physics Department, Faculty of Science, Tripoli University, Tripoli, Libya

Corresponding Author: E. S. Abd El-Halim

Abstract: Thirty samples of phosphate rocks were chosen to achieve this work. Samples were obtained from Quseir, Hamrawein, Safaga along Coast of the Red Sea, Egypt. Distributions of natural radionuclides of ²³⁸U, ²²⁶Ra, ²³²Th and ⁴⁰K in these samples were determined using a high-purity germanium detector (HPGe) with a specially designed shield. The content of uranium and radium is higher than permissible level in all samples, but the content of thorium and potassium is low. The activity ratios between Thorium to Uranium concentration for all phosphate samples were calculated (²³²Th/²³⁸U) (Clark value). The activity ratios ²³⁴U/²³⁸U, ²³⁰Th/²³⁸U, ²³⁰Th/²³⁴U, ²²⁶Ra/²³⁸U, ²³⁸U/²³⁵U and ²³⁴U/²³⁵U were calculated to estimate the radioactive equilibrium/disequilibrium in the area under study. In order to evaluate the radiological hazard from phosphate rocks in this area the radium equivalent activity (Ra_{eq}), absorbed gamma dose rate (D), annual effective dose equivalent (AEDE), external hazard index (H_{ex}) and excess lifetime cancer risk (ELCR) were calculated. In this work, the activity concentrations of Radon ²²²Rn, radon emanation factor, radon mass exhalation rate and annual effective dose from radon in these locations of the phosphate samples were calculated. This study reveals in general that all samples are exceeding the world permissible safe criteria and consider a risk source for human environment.

Keywords: Natural radionuclides, Phosphate rock, activity ratios, Health effects.

Date of Submission: 16-01-2019

Date of acceptance: 02-02-2019

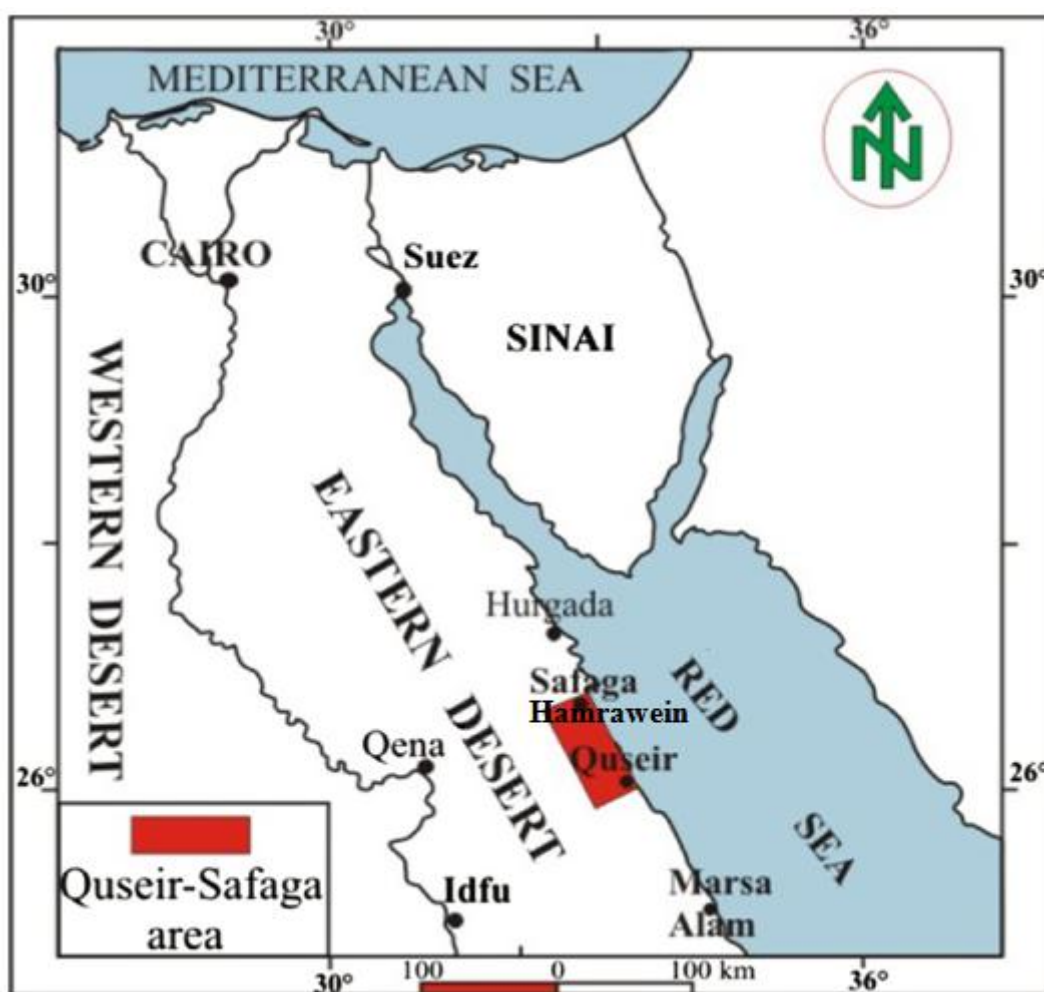
I. Introduction

Studies of natural environmental radiation and radioactivity are of great importance and interest for the environment as well as many other disciplines. Environmental radiation originates from a number of naturally occurring and human-made sources. The estimation of exposure to ionizing radiation is an important goal of regulatory authorities and radiation protection scientists. Thus knowledge of the background radiation level is of paramount importance (Dreketal., 2010). The distribution of radionuclides varies from area to another due to many reasons like the geological localities and natural chemical reactions as well as man activities. Study of natural radioactivity is usually done in order to gain information about the present levels of harmful pollutants discharged to the environment itself or in the living creatures. Phosphate ores of sedimentary origin have higher concentrations of radionuclides of the uranium family, the uranium concentration in the sampling region is more dependent upon the climatic effects, seasonal variability and the effects of evapotranspiration. Phosphate ores are present in the chemical form of calcium phosphates $Ca_3(PO_4)_2$ which are very old marine deposits associated with fossils. This form represents 85% of the worldwide production. The second type of phosphate materials is apatite that is igneous origin (El-Bahiet al., 2017). Phosphates are used extensively, as a source of phosphorus for fertilizers and for manufacturing phosphoric acid and gypsum. The use of phosphate fertilizers in agriculture and of gypsum in building materials is a further source of possible exposure to the public (Gaafar et al., 2016). Elevated radon exposure to the public can further be expected in sites being developed for housing (Vandenhove, 2000). The relative activities or abundance of a parent and daughter radioactive nuclei provide basic information about the type of equilibria and enrichment/depletion processes like the measured ratios of ²³⁴U/²³⁸U, ²²⁶Ra/²³⁸U, ²³⁰Th/²³⁸U, ²³⁰Th/²³⁴U and ²²⁶Ra/²³⁰Th. The phosphate deposits in Egypt are exposed in three major areas named: the Western Desert, the Nile Valley and along the Red Sea between Safaga and Quesir (Fig. 1). These deposits yield ore containing 90% phosphate and from 25 to 100 ppm uranium. Lesser importance are phosphate deposits in the Sinai Peninsula, which are of lower grade and considered to be commercially insignificant. The total phosphate reserves in Egypt are estimated to exceed 3 billion tons (Notholt, 1985). In this work, the activity concentration of ⁴⁰K, ²³⁸U, ²²⁶Ra and ²³²Th in some phosphate rock samples collected along the Red Sea between Quseir and Safaga are measured. Three locations of phosphate

mines have been selected for this study and they are from Safaga -Quseir. The results were used to assess the radiological hazard associated with the absorbed gamma dose rate D , the annual effective dose rate, radium equivalent activities (Ra_{eq}) and external hazard index (H_{ex}), also excessive lifetime cancer risk was calculated.

Geology of the study area

Quseir-Safaga area is located in the Central Eastern Desert of Egypt, between latitudes $25^{\circ} 58'$ and $26^{\circ} 22'$ N and longitudes $34^{\circ} 03'$ and $34^{\circ} 22'$ E (Fig 1). In the region of the Eastern Desert (Red Sea Coast) the phosphorite-bearing strata are known as the Duwi Formation. These beds rest with conformity on the Quseir variegated shale and are overlain by the deeper water marls and chinks of the Dakhla Formation (Fig. 2). The main phosphorite mineral is carbonate-fluorapatite (francolite). The non-phosphatic minerals are represented by dolomite, calcite, quartz, pyrite, goethite, gypsum, smectite, and kaolinite (Dabous, 2003). The clay minerals associated with Egyptian phosphorites occur mainly as a matrix or as a filling of the intergranular pores. Some clay minerals are also present as parts of the phosphatic pellets, or as fillings of the cavity-like microstructures in the bone and teeth fragments (Gaafaret al., 2016). The iron minerals goethite, hematite, and pyrite have been found as coatings on the outer surfaces of phosphate pellets and as parts of the cementing material.



Fig(1) Location map of Quseir-Safaga area along Red Sea, Egypt.

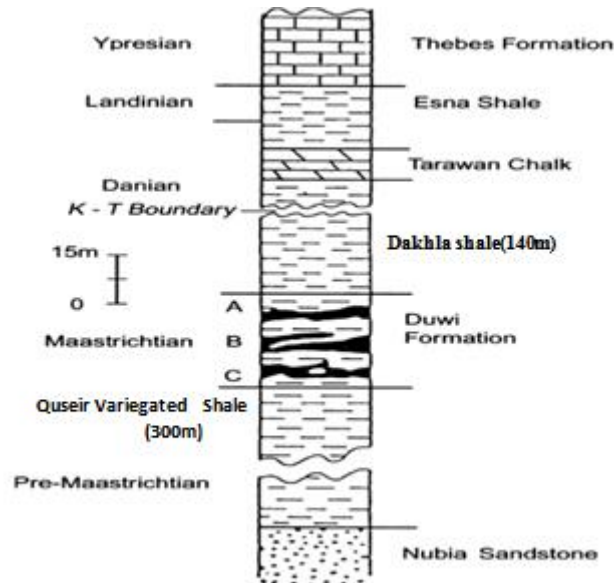


(Fig2)General stratigraphic column of the Quesir-Safaga district, showing the location of the phosphorite deposits. A, B, and C are the major phosphorite seams of the Duwi Formation in the Quesir-Safaga area(DABOUS,2003).

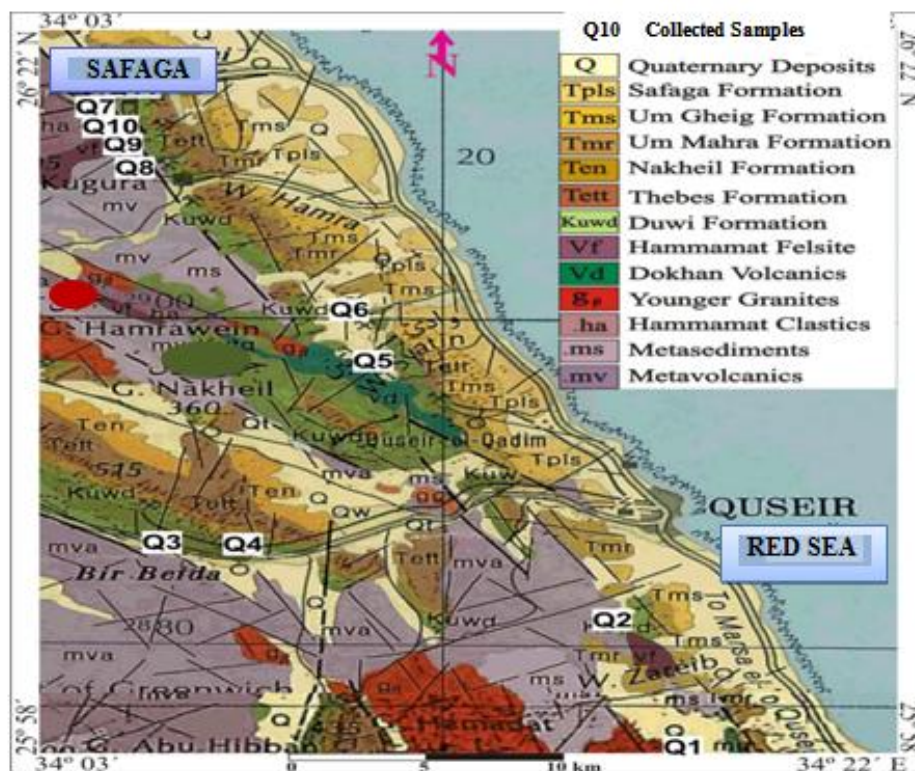


(Fig 3)Geologic map of Quseir-Safaga area, Central Eastern Desert, Egypt (Gaafaret *et al.*, 2016).

Experimental Procedures

Sampling and sample preparation

Three locations of open-pit phosphate mines have been selected for this study. These samples were collected by services partner, El-Quseir (34° 17' E 26° 05' N), El-Hamrawein (34° 10' E 26° 12' N) and Safaga (34° 06' E 26° 18' N) locations. Thirty samples from ten mines were collected, three samples from each mine, locations as in fig (3) samples from El-Quseir (Q1-Q4), El-Hamrawein (Q5-Q6), Safaga (Q7-Q10). The collected samples were transferred to labeled polyethylene bags, closed and transferred to the laboratory for preparation and measurements. The collected samples were dried at room temperature for a week, crushed and sieved through 200 mesh size. The quartering technique was used to get a representative sample for each horizon. Weighted

samples were placed in polyethylene bottles of 250 cm³ volume. The bottles were completely sealed for more than 4 weeks to allow radioactive equilibrium to be reached before measured by the gamma spectrometer. This step was necessary to prevent the escape of the radiogenic gas ²²²Rn. After that the samples were subjected to gamma-ray spectrometric analysis.

Procedure for gamma spectrometry

In the presentwork , a high – resolution gamma spectrometric system is used for the measurement of the energy spectrum of emitted gamma ray. The system consists of a high purity germanium (HPGe) detector coupled to a signal- processing units including a spectroscopy pulse amplifier and advanced multi-channel analyzer . The (HPGe) detector has resolution(FWHM) of 1.85KeV for the 1332.5KeV γ - ray line of ⁶⁰Co . The γ - ray spectrometer energy calibration was performed using ⁶⁰Co, ²²⁶Ra and ²⁴¹Am point sources. The detector was surrounded by a special heavy lead shield of about 10 cm thickness with inside dimension 28 cm diameter 40.5 cm height. The absolute detection efficiency of the HPGe detector was determined by using three well-known reference materials obtained from the International Atomic Energy Agency for U,Th and K activity measurements: RGU-1, RGTh-1 and RGK-1 (Abd El-Halim ,et al 2017) . The sample container was placed on top of the detector for counting. The same geometry and size were used for both the samples and the reference materials (Pekala et al., 2010). ²³⁸U was determined from the gamma rays emitted by its daughter products ²³⁴Th and ^{234m}Pa activities determined from the 63.3 and 1001 keV photo peaks, respectively, ²¹⁴Bi (609.3, 1120.3, 1238.1, 1377.7 and 1764.5 keV), ²¹⁴Pb (295.1 and 352.0 keV). The specific activity of ²²⁶Ra was measured using the 186.1 keV from its own gamma-ray (after the subtraction of the 185.7 keV of ²³⁵U). The specific activity of ²³²Th was measured using the 338.4, 911.2 and 968.9 keV lines from ²²⁸Ac and 583 keV peak from ²⁰⁸Tl, and ⁴⁰K was measured using 1460.8 keV peak. The measurement duration was up to 70000 sec. The obtained spectra were analyzed, in order to determine the background distribution due to naturally occurring radionuclides in the environment around the detector, an empty polyethelene container was counted in the same manner as the samples. The activity concentrations were calculated after measurement and subtraction of the background. The activities were determined from measuring their respective decay daughters. The activity concentrations were calculated from the intensity of each line taking into account the mass of the sample, the branching ratios of the γ -decay, the time of counting and the efficiencies of the detector (Papaefthymiou and Psichoudaki, 2008) .

II. Results and discussion

Activity Concentration

Activity concentration of ²²⁶Ra, ²³⁸U, ²³⁵U, ²³²Th and ⁴⁰K for phosphate rock samples were calculated as illustrated in (Table 1). The activity concentrations of ²³⁸U range from 341.39 to 1571.55 Bq/kg, ²³²Th from 9.63 to 16 Bq/kg, ²²⁶Ra from 643.98 to 2147 Bq/kg, ²³⁵U from 16.08 to 73.3 Bq/kg and ⁴⁰K from 75.84 to 138.38 Bq/kg. The radioelements worldwide average (W.A.) values are 33 Bq/kg for ²³⁸U, 32 Bq/kg for ²²⁶Ra, 45 Bq/kg for ²³²Th, 412 Bq/kg for ⁴⁰K and 33 Bq/kg for ²³⁵U (UNSCEAR, 2010) as shown in fig (4). The activity concentrations of all studied samples for radium, uranium are higher than the permissible level, but the activity concentrations of all studied samples for thorium and potassium are lower than the permissible level, the activity concentrations of most studied samples for ²³⁵U are higher than the permissible level except samples (Q1, Q2) are lower than the permissible level . Radium is the most dangerous decay product of uranium due to gaseous nature of its daughter radon , whose half-life is 3.8 days . During inhalation of phosphate dust , the alpha particles emanating from radon induce radiation damages to lungs. These results indicate an increase in radium activity concentration. Actual radionuclide concentrations will vary in location because of varying geological characteristics of phosphate ores in different regions.

(Table 1) The activity concentration of ²²⁶Ra, ²³⁸U, ²³⁵U, ²³²Th and ⁴⁰K (in Bq/kg) of the phosphate samples.

| Locality | Sample | ²²⁶ Ra | ²³⁸ U | ²³⁵ U | ²³² Th | ⁴⁰ K |
|-----------|--------|-------------------|------------------|------------------|-------------------|-----------------|
| | Q1 | 726.72 | 341.39 * | 16.08* | 16 | 116.41 |
| Quseir | Q2 | 643.98* | 495.26 | 23.52 | 10.66 | 138.38** |
| | Q3 | 1080 | 840.37 | 38.78 | 13.02 | 97.36 |
| | Q4 | 1776 | 1320.04 | 61.34 | 14.29 | 75.84* |
| | Q5 | 2147** | 1569.91 | 73.3** | 9.63 * | 131.5 |
| Hamrawein | Q6 | 1364 | 980.41 | 45.61 | 14.36 | 109.5 |
| | Q7 | 964.81 | 804.62 | 37.63 | 14.51 | 112.6 |
| Safaga | Q8 | 1885 | 1374.22 | 65.03 | 13.3 | 87.25 |
| | Q9 | 2076 | 1121.97 | 51.39 | 16** | 89.92 |
| | Q10 | 1843 | 1571.55 ** | 72.5 | 16 | 88.73 |
| P.L | | 32 Bq/kg | 33Bq/kg | 33Bq/kg | 45Bq/kg | 412Bq/kg |

* The lower value. ** The higher value

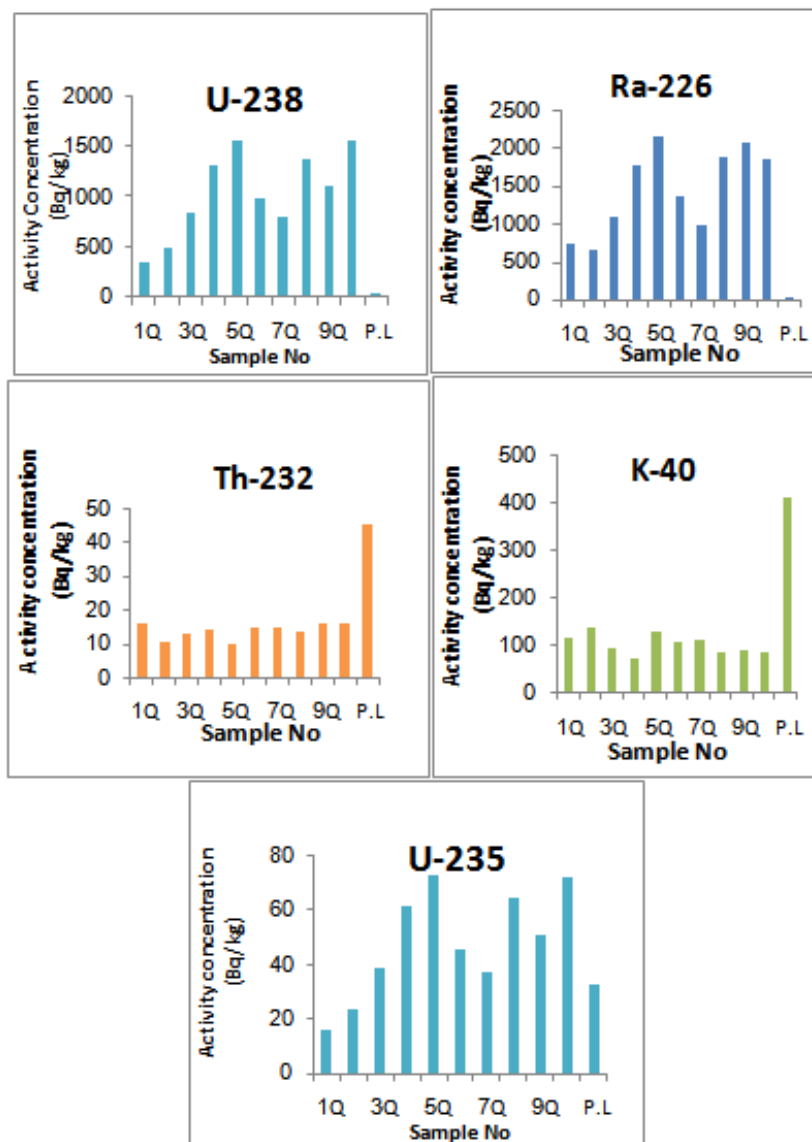


(Fig4)The activity concentrations for ^{238}U , ^{235}U , ^{226}Ra , ^{232}Th , ^{40}K in the phosphate samples in comparison with the permissible level (p.l.).

In this work the concentration of ^{238}U and ^{232}Th in phosphate samples (in ppm) and activity ratio $^{232}\text{Th}/^{238}\text{U}$ were calculated and illustrated in (table 2). The concentrations of ^{238}U range between 27.53 and 126.6 ppm, and ^{232}Th between 2.37 and 3.94 ppm, while the $^{232}\text{Th}/^{238}\text{U}$ ratios range between 0.01 and 0.14 which is lower than the Clark's value (3.5).

(Table 2)The ^{238}U and ^{232}Th concentration in phosphate samples (in ppm) and $^{232}\text{Th}/^{238}\text{U}$ ratio.

| Locality | Samples | ^{238}U | ^{232}Th | $^{232}\text{Th}/^{238}\text{U}$ |
|-----------|---------|------------------|-------------------|----------------------------------|
| Quseir | Q1 | 27.53* | 3.94** | 0.14** |
| | Q2 | 39.94 | 2.62 | 0.06 |
| | Q3 | 67.77 | 3.2 | 0.04 |
| | Q4 | 106.45 | 3.51 | 0.03 |
| | Q5 | 126.6** | 2.37* | 0.01* |
| Hamrawein | Q6 | 79.06 | 3.53 | 0.04 |
| | Q7 | 64.88 | 3.57 | 0.05 |
| Safaga | Q8 | 110.82 | 3.27 | 0.02 |
| | Q9 | 90.48 | 3.94 | 0.04 |
| | Q10 | 126.73 | 3.94 | 0.03 |

* The lower value. ** The higher value.

Activity Ratios

The basic rule of U-disequilibrium study is that after a period of time of about 5-6 half-lives of daughter, the parent and the daughter will have similar activities if there is no disturbance in the system (secular equilibrium). If there is a disturbance by any process resulting in a net removal or addition of either of the two, the activity ratio is no longer unity but departs from the equilibrium value to an extent that depends on the characteristics of the disturbance process. This is the state of disequilibrium. Disequilibrium between ^{238}U and ^{234}U in natural waters and sediments is a common phenomenon. Mechanisms responsible for such disequilibrium include α -particle recoil ejection of ^{234}Th (a precursor of ^{234}U) (fig.5) into solution. This process led to facilitating the solubility of this isotope. Therefore, the $^{234}\text{U}/^{238}\text{U}$ activity ratios of surface or groundwaters are usually greater than unity (Dawood, 2010). Physical processes involve α -recoil while chemical processes involve leaching through either acidic or alkaline solutions. Although ^{234}U and ^{238}U are chemically of the same behavior, they also exhibit fractionation due to physical process. As a result of alpha particle emission from the parent ^{238}U , the recoiled ^{234}U is added to the water.

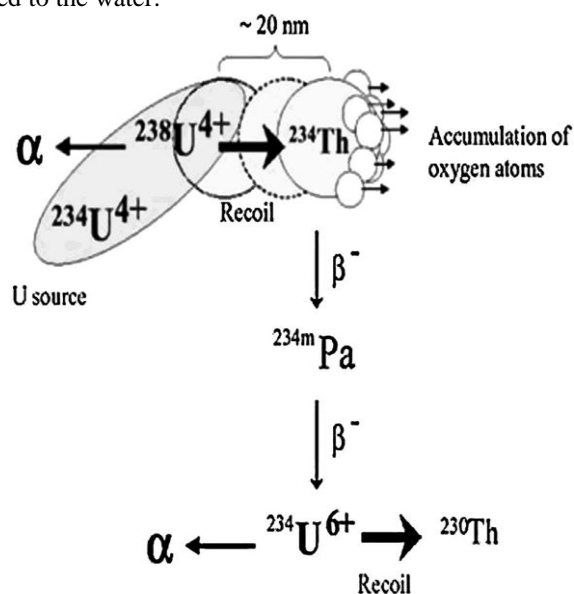


(Fig 5) A conceptual model of physical and chemical events when ^{238}U decays to ^{234}U (El-Aassyet al., 2015).

The activity ratios $^{226}\text{Ra}/^{238}\text{U}$ were calculated for all rock phosphate samples (see Table 3) which show disequilibrium between ^{226}Ra and ^{238}U (1.2 -2.12). The activity ratios $^{234}\text{U}/^{238}\text{U}$ for all samples show equilibrium around unity except Q8 greater than unity and deviating from secular equilibrium. High value of ^{234}U isotope than ^{238}U may be due to alpha recoil phenomenon (physical model) as shown in fig 5, Another is related to the chemically unstable state (chemical model). The activity ratios of $^{230}\text{Th}/^{234}\text{U}$ and $^{230}\text{Th}/^{238}\text{U}$ (Table 3) for most samples are showed equilibrium around unity, except (Q8, Q9, Q10) lower than unity. Where the activity ratios ($^{226}\text{Ra}/^{238}\text{U} > 1$), ($^{230}\text{Th}/^{238}\text{U}$ and $^{230}\text{Th}/^{234}\text{U} < 1$) for sample Q8 show in (Table 3) which indicating preferential migration in/ or accumulation of uranium. The $^{238}\text{U}/^{235}\text{U}$ activity ratio for all phosphate samples vary between 21.05 and 21.83 (Table 3) which reflect little deviation from the normal ratio (21.7) as shown in figure (6). The value of ratio $^{234}\text{U}/^{235}\text{U}$ in Table (3) is varied between 19.18 and 29 which mean uranium leaching out from sample due to alteration processes showed in figure (7).

(Table 3) Activity ratios of Phosphate samples at Quseir-Hamrawein-Safaga area, Egypt.

| Locality | Sample | $^{238}\text{U}/^{235}\text{U}$ | $^{234}\text{U}/^{235}\text{U}$ | $^{234}\text{U}/^{238}\text{U}$ | $^{230}\text{Th}/^{238}\text{U}$ | $^{230}\text{Th}/^{234}\text{U}$ | $^{226}\text{Ra}/^{238}\text{U}$ |
|-----------|---------|---------------------------------|---------------------------------|---------------------------------|----------------------------------|----------------------------------|----------------------------------|
| Quseir | Q1 | 21.22 | 20.27 | 0.95 | 1.03 | 1.07 | 2.12 |
| | Q2 | 21.05 | 19.18 | 0.91 | 0.81 | 0.89 | 1.3 |
| | Q3 | 21.66 | 23.62 | 1.09 | 1 | 0.92 | 1.3 |
| | Q4 | 21.52 | 21.79 | 1.01 | 1.04 | 1.03 | 1.3 |
| | Average | 21.36 | 21.21 | 0.99 | 0.97 | 0.97 | 1.5 |
| Hamrawein | Q5 | 21.41 | 24 | 1.12 | 0.86 | 0.76 | 1.4 |
| | Q6 | 21.49 | 20.74 | 0.96 | 0.93 | 0.96 | 1.4 |
| | Average | 21.45 | 22.37 | 1.04 | 0.89 | 0.86 | 1.4 |
| Safaga | Q7 | 21.38 | 19.32 | 0.9 | 0.81 | 0.9 | 1.2 |
| | Q8 | 21.13 | 29 | 1.4 | 0.78 | 0.56 | 1.4 |
| | Q9 | 21.83 | 21.61 | 0.98 | 0.48 | 0.49 | 1.9 |
| | Q10 | 21.66 | 22.11 | 1.02 | 0.53 | 0.52 | 1.2 |
| | Average | 21.5 | 23.01 | 1.07 | 0.65 | 0.61 | 1.42 |

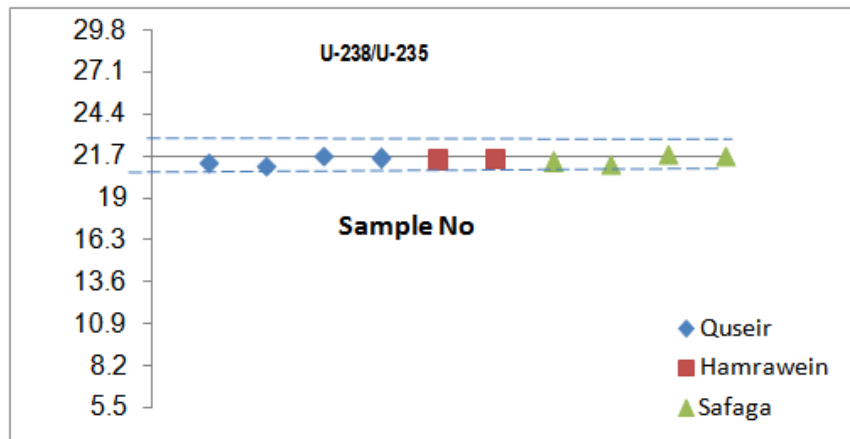


(Fig 6) Variations of the $^{238}\text{U}/^{235}\text{U}$ activity ratio in studied samples. The certified value is 21.7 .

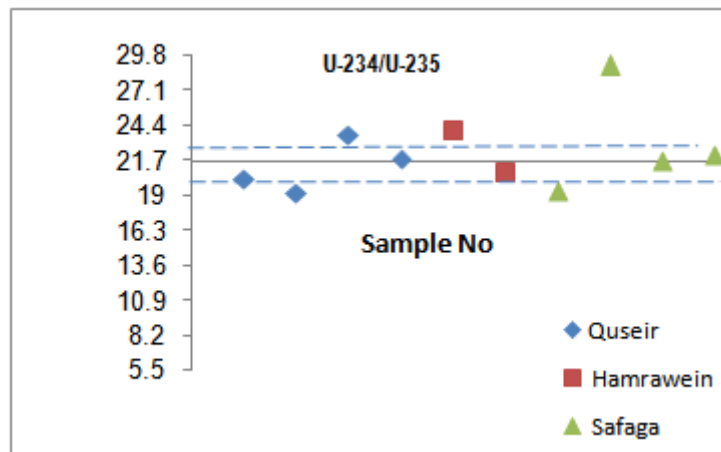


(Fig 7) Variations of the $^{234}\text{U}/^{235}\text{U}$ activity ratio in studied samples. The certified value is 21.7 .

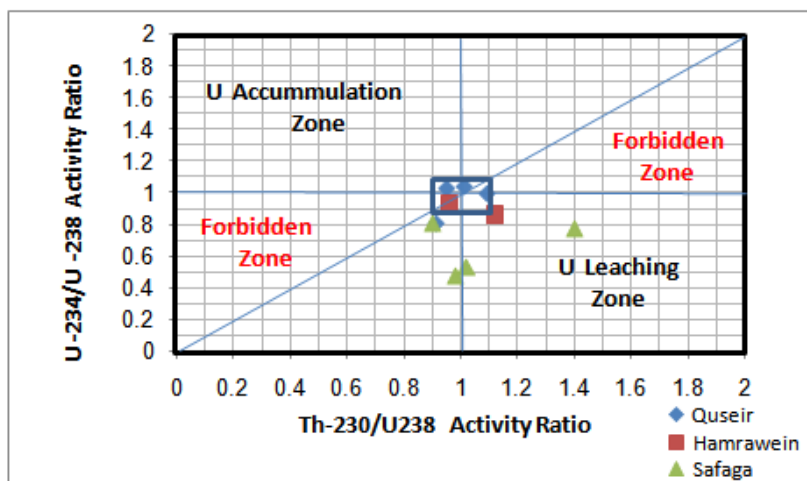


(Fig 8) Schematic diagram showing the evolution of $^{234}\text{U}/^{238}\text{U}$ versus $^{230}\text{Th}/^{238}\text{U}$ activity ratios for all phosphate samples at Quseir- Hamrawein- Safaga area.

In a plot of $^{234}\text{U}/^{238}\text{U}$ versus $^{230}\text{Th}/^{238}\text{U}$ (Fig. 8), the pathways of return to equilibrium for solid phases are shown for two cases: accumulation of U ($^{230}\text{Th}/^{238}\text{U}$ decrease) and leaching of U ($^{230}\text{Th}/^{238}\text{U}$ increase) as samples (Q2, Q5, Q7, Q8, Q9 and Q10). The presence of data points in the forbidden zones may be explained as a result of continuous and contrasting U mobilization processes. Depending on the relative rates of U gains and

losses and on the intensity of the Ufractionation, it is possible to explain the data points present in the forbidden zone.

According to judging standards, activity ratios between 0.90 and 1.10 are referred as secular equilibrium within the conservative (10 %) analytical error for the samples. It is supported by the Thiel diagram (Fig. 8), in which the samples that plot into the boxed-in area (Q1, Q3, Q4, Q6) are reconsidered near or at secular radioactive equilibrium. Plots of the samples deviating from secular equilibrium, i.e., larger than 1.10 or less than 0.90 for $^{234}\text{U}/^{238}\text{U}$, $^{230}\text{Th}/^{238}\text{U}$, $^{230}\text{Th}/^{234}\text{U}$ and $^{226}\text{Ra}/^{230}\text{Th}$, fall into the forbidden region in the Thiel diagram (Fig. 8), a complex geochemical region where the systems can be identified as having suffered complicated U migration. A complex leaching and accumulation of uranium might take place (Abdel Gawad and Ibrahim, 2015).

Radiological hazard indices

Radium Equivalent (R_{eq}):

Radium equivalent (R_{eq}) index in Bq/kg is a widely used radiological hazard index. It is a convenient index to compare the specific activities of samples containing different concentrations of ^{226}Ra , ^{232}Th and ^{40}K . It was defined on the assumption that 10 Bq/kg of ^{226}Ra , 7 Bq/kg of ^{232}Th and 130 Bq/kg of ^{40}K produce the same gamma dose rate. It was calculated as follows.

$$R_{eq} = C_{Ra} + 1.43 C_{Th} + 0.077 C_K \dots \dots \dots (1)$$

Where C_{Ra} , C_{Th} and C_K are the activity concentrations of ^{226}Ra , ^{232}Th and ^{40}K in Bq/kg, respectively. R_{eq} was estimated for the collected samples and are given in Table (4). The values of R_{eq} for all phosphate samples varied (from 669.88 to 2170.9) Bq kg⁻¹, were estimated higher than the recommended maximum value of 370 Bq kg⁻¹ (Ababneh et al., 2010).

External Hazard Index (H_{ex}):

The external hazard index (H_{ex}) represents the external radiation exposure associated with gamma irradiation from radionuclides of concern. The value of H_{ex} should not exceed the maximum acceptable value of one in order to keep the hazard insignificant. The external hazard index (H_{ex}) is defined by equation (Jankovic et al., 2008):

$$H_{ex} = (C_{Ra}/370 + C_{Th}/259 + C_K/4810) \leq 1 \dots \dots \dots (2)$$

Where C_{Ra} , C_{Th} and C_K are the concentration in (Bq Kg⁻¹) of radium, thorium and potassium respectively. The values of H_{ex} for all phosphate samples varied from (1.81-5.86), were found to be more than 1 given in Table (4).

Radiation Level Index (I_γ):

This index can be used to estimate the level of γ -radiation hazard associated with the natural radionuclides in the samples; it is given by the equation

$$I_\gamma = C_{Ra}/150 + C_{Th}/100 + C_K/1500 \dots \dots \dots (3)$$

Where C_{Ra} , C_{Th} and C_K are the activity concentration of ^{226}Ra , ^{232}Th , ^{40}K in Bq/kg, respectively. The value of these indexes must be less than unity in order to keep the radiation hazard insignificant, the values of Representative Level

Index (I_γ) from (4.49 -14.49) for all samples are found to be more than 1 given in Table (4).

Absorbed Dose Rate D:

The absorbed gamma dose rates in air at 1 m above the ground surface for the uniform distribution of radionuclides (^{238}U , ^{232}Th and ^{40}K) were calculated by equation :

$$D = 0.427 * C_U + 0.662 * C_{Th} + 0.043 * C_K \text{ (nGy/h)} \dots \dots \dots (4)$$

where C_U , C_{Th} and C_K are the activity concentration of ^{238}U , ^{232}Th and ^{40}K in Bq/kg, respectively. The range of absorbed dose rate in the samples due to natural radionuclides is (161.34–685.42) nGy h⁻¹ given in Table (4). The values of the Dose rate calculated during present study are found higher than the permissible level of 59 nGy/h (Abd El-Halim et al., 2017).

The annual outdoor effective dose (E_{out}) is estimated from the outdoor external dose rate (D_{out}), time of stay in the outdoor or occupancy factor (OF = 20 % of 8760 h in a year) and the conversion factor (CF = 0.7 Sv.Gy⁻¹) to convert the absorbed dose in air to effective dose. During the present study, the E_{out} was calculated using the following equations from (UNSCEAR, 2010):

$$E_{out} = D_{out} \text{ (nGy h}^{-1}\text{)} * 0.2 * 8760 \text{ h} * 0.7 \text{ (Sv * Gy}^{-1}\text{)} \dots \dots \dots (5)$$

the outdoor effective dose rate E_{out} range from (0.19 to 0.84 mSv/y), the values of the all studied samples listed (in table 4) are found higher than the world's average 0.07 mSv/y.

Excess lifetime cancer risk (ELCR) :

The value of annual effective dose excess lifetime cancer risk (ELCR) was calculated by using the equation :

$$ELCR_{out} = E_{out} * LE * RF \dots\dots\dots(6)$$

Where E_{out} is the annual effective dose, LE life expectancy (66 years) and RF (Sv^{-1}) is risk factor per Sievert, which is 0.05 .The values of $ELCR_{out}$ range between (652.75×10^{-3} and 2773.11×10^{-3})in the phosphate samples Table (4).All values are higher than the permissible level $0.29 * 10^{-3}$ (**Qureshiet al ., 2014**).

(Table4) The values of radium equivalent (Bq/kg), radioactivity level index , external hazard, the outdoor absorbed rate (nGy/h), outdoor annual effective dose (mSv/y)and outdoor Excess lifetime cancer risk atQuseir-Hamrawein - Safaga,Egypt .

| Locality | Sample | Ra _{eq} (Bq/kg) | I _γ (Bq/kg) | H _{ex} (Bq/kg) | D _(out) (nGy/h) | E _{eff(out)} (mSv/y) | ELCR _(out) *10 ⁻³ |
|-----------|--------|-----------------------------|---------------------------|----------------------------|-------------------------------|----------------------------------|--|
| Quseir | Q1 | 758.56 | 5.08 | 2.05 | 161.34* | 0.19* | 652.75* |
| | Q2 | 669.88* | 4.49 * | 1.81* | 224.46 | 0.27 | 908.13 |
| | Q3 | 1106.12 | 7.39 | 2.98 | 371.62 | 0.45 | 1503.51 |
| | Q4 | 1802.27 | 12.03 | 4.87 | 576.35 | 0.706 | 2331.79 |
| Hamrawein | Q5 | 2170.9** | 14.49** | 5.86** | 682.36 | 0.83 | 2760.71 |
| | Q6 | 1392.97 | 9.31 | 3.76 | 432.82 | 0.53 | 1751.13 |
| Safaga | Q7 | 994.22 | 6.65 | 2.68 | 357.99 | 0.43 | 1448.36 |
| | Q8 | 1910.73 | 12.75 | 5.16 | 599.32 | 0.73 | 2424.74 |
| | Q9 | 2105.8 | 14.05 | 5.69 | 493.51 | 0.60 | 1996.65 |
| | Q10 | 1872.71 | 12.5 | 5.06 | 685.42** | 0.84** | 2773.11 ** |
| P.L | | 370 Bq/kg | unity | unity | 59 nGyh-1 | 0.07 mSvy ⁻¹ | 0.29*10 ⁻³ |

*The lowest value

**The highest value

(Table 5) The values of the activity concentration of radon ²²²Rn (Bq/m³), radon emanation factor, radon mass exhalation rate and the annualeffective dose from radon (AED_{Rn}) in the Phosphate samples atQuseir-Hamrawein - Safaga , Egypt .

| Locality | Sample | Ra-226 Bq/kg | Pb-214 Bq/kg | F _{Rn} | ²²² Rn (Bq/m ³) | E _{Rn} (mBq/kg.s) | AED _{Rn} (msv/y) |
|-----------|--------|-----------------|-----------------|-----------------|---|-------------------------------|------------------------------|
| Quseir | Q1 | 726.72 | 515.37 | 0.29 | 2056.43 | 0.44 | 14.12 |
| | Q2 | 643.97* | 453.82* | 0.29 | 1850.21* | 0.39* | 12.7 * |
| | Q3 | 1080 | 791.88 | 0.26 * | 2803.4 | 0.6 | 19.25 |
| | Q4 | 1776 | 1240 | 0.3 | 5215.28 | 1.12 | 35.81 |
| Hamrawein | Q5 | 2147** | 1366** | 0.36 | 7599.13 | 1.64 | 52.19 |
| | Q6 | 1364 | 913.17 | 0.33 | 4386.57 | 0.94 | 30.12 |
| Safaga | Q7 | 964.81 | 682.75 | 0.29 | 2744.44 | 0.59 | 18.84 |
| | Q8 | 1885 | 971.8 | 0.48 | 8885.43 | 1.91 | 61.02 |
| | Q9 | 2076 | 968.43 | 0.53** | 10776.65** | 2.32** | 74.01 ** |
| | Q10 | 1843 | 1234 | 0.33 | 5925.57 | 1.27 | 40.69 |

The lowest value

**The highest value

Radon Exhalation Rates

The Radon mass exhalation rates the emanation rate coefficient and the fraction of ²²²Rn that can diffuse through the raw and building materials is known as the emanation coefficient. The emanation coefficient (C_{Rn}) is a very important radiological index that can be used to evaluate the amount of the ²²²Rn emanated fraction released from the building raw materials and products containing, naturally occurring radionuclides such as ²²⁶Ra in radioactivity equilibrium with its parents. The emanation rate is estimated by measuring gamma rays from the radon decay daughter products, ²¹⁴Pb or ²¹⁴Bi. Assuming an equilibrium state :C_{Ra}= C_D+ C_{Rn}.....(7)

Where C_{Ra} is the measured activity of ²²⁶Ra, C_D is the measured activity of the daughter elements ²¹⁴Pb (or ²¹⁴Bi) and C_{Rn}is the estimated activity of ²²²Rn, which escapes into the surrounding environment.C_{Rn}can be expressed through the introduction of the radon emanation factor F, which is defined as (**Ioannides et al., 1997**).

$$C_{Rn} = (C_{Ra} - C_D) \times \rho \dots\dots\dots(8)$$

Where ρ is the density of radon (9.73 kg.m⁻³), The introduction of the radon factor F, which is defined as :

$$F = \frac{C_{\epsilon}}{C_{Ra}} = \frac{C_{Ra} - C_D}{C_{Ra}} \dots \dots \dots (9)$$

The mass exhalation rate or radon mass exhalation rate is the product of the emanation factor and ²²²Rn production rate (Seref and Lüfullah., 2008) , the mass exhalation rate (E_{Rn} in Bq/Kg.S) was determined by the following equation:

$$E_{Rn} = F_{Rn} \cdot A_{Ra} \cdot \lambda_{Rn} \dots \dots \dots (10)$$

Where: A_{Ra} is the specific activity of ²²⁶Ra (Bq/Kg) and λ_{Rn} is the decay constant of ²²²Rn (2.1×10⁻⁶ S⁻¹). Radon concentration was converted in to an effective dose, because the long standing exposure to high concentration of radon and its progenies may lead to pathological effects like lung cancer. The effective dose received by workers due to inhalation of radon gas and its decay products, where calculated by relation [ICRP, 1993] :

$$AED_{Rn} = \frac{C_{Rn} \times 0.4 \times K \times H}{3700 \text{ Bq.m}^{-3} \times 170 \text{ h}} \dots \dots \dots (11)$$

Where AED_{Rn} is the annual effective dose (mSv.y⁻¹), C_{Rn} is the emanation coefficient of radon (Bq.m⁻³), K is the ICRP dose conversion factor (5 mSv WLM⁻¹ for occupational worker and 3.88 mSv WLM⁻¹ for general public), H is the annual occupancy at the location 2160 h for workers and 7000 h for residents (80 % of total time) and 170 is exposure hours taken for WLM⁻¹ (Work Limit in Month)(Nikl and vegvari,1992). Table (5) represents the activity concentration of ²²²Rn, radon emanation factor F, radon mass exhalation rate and the annual effective dose from radon (AED_{Rn}). The activity concentrations of ²²²Rn were varied between (1850.21– 10776.65) Bq/m³, the highest value of activity concentration of ²²²Rn appear in the sample Q9, but the lowest value ²²²Rn appear in the sample Q2 . The values of the radon emanation factor and the radon mass exhalation rate of the samples are ranged from (0.26 to 0.53) and (0.39 to 2.32) mBq/Kg.s, respectively. The lowest value of the radon mass exhalation rate represent in Q2 while the highest value in the sample Q9 . The annual effective dose from radon AED_{Rn} in the samples ranged between (12.7 – 74.01) mSv/y, the highest value appears in the sample Q9, but the lowest value appears in the sample Q2. The results indicate high levels of annual effective dose from radon in Safaga locality. All the samples in this locality were higher than the maximum permissible dose limits (10 mSv) recommended by (ICRP, 1993).

III. Conclusions

The activity concentrations of ²³⁸U, ²²⁶Ra for all phosphate samples at Quseir Hamrawein-Safaga area are higher than the world's average , while The activity concentrations of ²³²Th and ⁴⁰K are low . All the phosphate samples have the ²³²Th/²³⁸U ratio less than the Clark's value (3.5) . The activity ratios ²²⁶Ra/²³⁸U showed a state of disequilibrium between the most of samples. While the activity ratios between ²³⁴U/²³⁸U for the most of samples are in the trend of U migration out equilibrium state. Activity ratios ²³⁰Th/²³⁴U and ²³⁰Th/²³⁸U found greater than unity, which is consistent with the preferential mobilization of uranium from the phosphate by leaching process. The radium equivalent and external hazard index , dose rate have high values. The ELCR factor assessed during this work on the basis of outdoor effective dose (E_{out}) was found to be higher than the permissible level. The activity concentrations of Radon ²²²Rn, radon emanation factor and radon mass exhalation rate of the samples were calculated. The obtained measurements indicate high levels of annual effective dose from radon in these locations. All the studied samples are higher than the maximum permissible dose limits (10 mSv). This may indicate that the workers in the mines of phosphate receive higher total effective doses due to high radioactivity, and the workers in these locations must be taken possible precautions and protection against the high radioactivity to reduce the risk. The results of measurements will serve as base line data and background reference level for Egyptian coastlines.

References

- [1]. Ababneh Z.Q, El-Omari ,H . Rasheed, M . El-Najjar T. and A. Ababneh, (2010) "Assessment of gamma emitting radionuclides in sediment cores from the Gulf of Aqaba", Red Sea. Radiat Prot Dosim., vol. 141, pp. 289-298.
- [2]. Abd El – Halim E.S, Sroor A , El-Bahi S M , Ibrahim E. El – Aassy , Enass M. El Shaikh and Musa K.M. (2017) "Assessment of Radioactivity levels and hazards for some sedimentary rock samples in different localities southwestern , Sinai ,Egypt" International Journal of Recent Scientific Research Vol.8, Issue,11, pp.21916-21922, November, 2017.
- [3]. Abd El-Halim E. S. , Walley El-Dine N, El-Bahi S.M, El-Aassy I.E, El-Sheikh E.M, Al-Abrdi A.M (2017) " Excessive lifetime cancer risk and natural radioactivity measurements of granite and sedimentary rock samples " ISSN 1818-331X ,T. 18 № 4.
- [4]. Abdel Gawad E. and Ibrahim E.M., (2015): "Activity Ratios as a Tool for Studying Uranium Mobility at El Sela Shear Zone, Southeastern Desert, Egypt", *JRadioanal Nucl Chem*, DOI 10.1007/s10967-015-4374-0.
- [5]. Dabous ,A. A (2003) , Secondary uranium in phosphorites and its relation to groundwater in Egypt , *Geochemical Journal*, Vol. 37, pp. 413 to 426.
- [6]. Dawood H .(2010) "Factors Controlling Uranium and Thorium Isotopic Composition of the Stream bed Sediments of the River Nile , Egypt" *JAKU :Earth Sci* , Vol.21, No2, pp:77-103 .
- [7]. Drek H.C, May C.C and Zanat C., 2010: Global networking for Biodosimetry laboratory capacity in radiation emergencies. *Health phys.* 92(2): P,168.

- [8]. EL-Aassy I. E , El-Feky M. G , Issa F. A. , Ibrahim N. M , Desouky O. A ,Khattab M. R (2015) " Uranium and $^{234}\text{U}/^{238}\text{U}$ isotopic ratios in some groundwater wells at southwestern Sinai , Egypt " J RadioanalNuclChem (2015)303:357-362.
- [9]. El-Bahi S.M , Sroor A, GehanY,Mohamed , El-Gendy N.S(2017) "Radiological impact of natural radioactivity in Egyptian phosphate rocks, phosphogypsum and phosphate fertilizers" Applied Radiation and Isotopes 123, 121-127.
- [10]. GaafarI,El-Shershaby A , Zeidan I and El-Ahll, L .(2016) "Natural radioactivity and radiation hazard assessment of phosphate mining, Quseir-Safaga area, Central Eastern Desert, Egypt" NRIAG Journal of Astronomy and Geophysics 5, 160–172.
- [11]. ICRP International Commission on Radiological Protection, (1993), "Protection against radon-222 at home and work, ICRP Publication 65. Oxford: Pentagon press .
- [12]. Ioannides K. G, Mertzimekis T. J, Papachristodoulou C. A and Tziolla C. E., (1997), "Measurements of Naturalradioactivity in phosphate fertilizers"Science of The Total Environment ,Volume 196, Issue 1, 9 March 1997, Pages 63-67 .
- [13]. Jankovic, M .Todorovic,D and Savanovic ,M (2008)"Radioactivity measurements in soil samples collected in the Republic of Srpska", Radiation Measurements, vol. 43, pp. 1448-1452.
- [14]. Nikl I. and Vegvari. I, (1992) "The Natural radioactivity of coal and by products in Hungarian Coal Fired Power Plants", IzotopetchnikaDiagnosztika, V 35, pp. 57-64.
- [15]. Notholt, A. J. G. (1985) Phosphorite resources in the Mediterranean TethyanPhosphogenic Province: Aprogress report. *Sciences Geologiques Memoir* 77, 9–21.
- [16]. Papaefthymiou, H. and Psychoudaki, M. (2008) Natural Radioactivity Measurements in the City of Ptolemais (Northern Greece). *Journal of Environmental Radioactivity*, 99, 1011-1017. <http://dx.doi.org/10.1016/j.jenvrad.2007.12.001>
- [17]. Pekala M, Kramers JD and Waber HN (2010): " $^{234}\text{U}/^{238}\text{U}$ Activity Ratio Disequilibrium Technique for Studying Uranium Mobility in the Opalinus Clay at Mont Terri, Switzerland". *ApplRadiatIsot*68:984-992.
- [18]. QureshiA . A , Tariq S , Ud Din K , ManzoorS,CalligarisC,Waheed A(2014) " Evaluation of excessive lifetime cancer risk due to natural radioactivity in the rivers sediments of Northern Pakistan". *Journal of Radiation Research and Applied Science* 7 , 438-447.
- [19]. SerefTurhan and LüfullahGunduz., (2008), "Determination f Specific Activity of ^{226}Ra , ^{232}Th and ^{40}K for Assessment of Radiation Hazards from Turkish Pumice Samples", *Journal of Environmental Radioactivity*, Vol. 99, P. 332-342.
- [20]. UNSCEAR, 2010. Sources and Effects of Ionizing Radiation. Report to General Assembly with Scientific Annexes (New York, United Nations Scientific Committee on the Effect of Atomic Radiation).
- [21]. Vandenhove, H., 2000. European sites contaminated by residues from the ore extracting and processing industries. In: Proceedings Series, STI/PUB/1092, IAEA, Vienna, pp. 61–89.

IOSR Journal of Applied Physics (IOSR-JAP) is UGC approved Journal with Sl. No. 5010, Journal no. 49054.

E. S. Abd El-Halim "Radiological impact of natural radioactivity and excessive lifetime cancer risk in Egyptian phosphate rocks along Red Sea, Egypt." *IOSR Journal of Applied Physics (IOSR-JAP)* , vol. 11, no. 1, 2019, pp. 47-57.